Phosphoinositide 3–kinase γ participates in T cell receptor–induced T cell activation

Isabela Alcázar,[1] Miriam Marqués,[1] Amit Kumar,[1] Emilio Hirsch,[2] Matthias Wymann,[3] Ana C. Carrera,[1] and Domingo F. Barber[1]

[1]Department of Immunology and Oncology, Centro Nacional de Biotecnología (CNB)/Consejo Superior de Investigaciones Cientificas, Madrid 28049, Spain
[2]Department of Genetics Biology and Biochemistry, Center for Molecular Biotechnology, University of Torino, 10126 Turin, Italy
[3]Department of Clinical and Biological Sciences, Institute of Biochemistry and Genetics, University of Basel, 4058 Basel, Switzerland

Class I phosphoinositide 3–kinases (PI3Ks) constitute a family of enzymes that generates 3-phosphorylated polyphosphoinositides at the cell membrane after stimulation of protein tyrosine (Tyr) kinase–associated receptors or G protein–coupled receptors (GPCRs). The class I PI3Ks are divided into two types: class I_A p85/p110 heterodimers, which are activated by Tyr kinases, and the class I_B p110γ isoform, which is activated by GPCR. Although the T cell receptor (TCR) is a protein Tyr kinase–associated receptor, p110γ deletion affects TCR-induced T cell stimulation. We examined whether the TCR activates p110γ, as well as the consequences of interfering with p110γ expression or function for T cell activation. We found that after TCR ligation, p110γ interacts with $G\alpha_{q/11}$, lymphocyte-specific Tyr kinase, and ζ-associated protein. TCR stimulation activates p110γ, which affects 3-phosphorylated polyphosphoinositide levels at the immunological synapse. We show that TCR-stimulated p110γ controls RAS-related C3 botulinum substrate 1 activity, F-actin polarization, and the interaction between T cells and antigen-presenting cells, illustrating a crucial role for p110γ in TCR-induced T cell activation.

CORRESPONDENCE
Domingo F. Barber:
dfbarber@cnb.uam.es

Abbreviations used: CXCR, CXC chemokine receptor; GPCR, G protein–coupled receptor; IS, immunological synapse; ITAM, immunoreceptor Tyr-based activation motif; Lck, lymphocyte-specific Tyr kinase; MAPK, mitogen-activated protein kinase; PCC, pigeon cytochrome c; PH, pleckstrin homology; PI3K, phosphoinositide 3–kinase; PIP_2, phosphatidylinositol-3,4-biphosphate; PIP_3, phosphatidylinositol-3,4,5-trisphosphate; PKB, protein kinase B; Rac1, RAS-related C3 botulinum substrate 1; SEE, staphylococcal enterotoxin E; SH2, Src homology 2; Tg, transgenic; TRIM, TCR-interacting molecule; Tyr, tyrosine; ZAP70, ζ-associated protein.

Receptor-regulated class I phosphoinositide 3–kinases (PI3Ks) are lipid kinases that produce phosphatidylinositol-3,4,5-trisphosphate (PIP_3) and phosphatidylinositol-3,4-biphosphate (PIP_2) at the plasma membrane. These lipids act as second messengers by recruiting proteins containing pleckstrin homology (PH) domains to cell membranes, thereby initiating various cell responses. The PI3Ks are classified as class I_A and I_B, according to their mode of activation. Class I_A PI3Ks are activated downstream of tyrosine (Tyr) kinase–associated receptors (1, 2), whereas class I_B is activated by G protein–coupled receptors (GPCRs), which include the chemokine receptors (3). Class I_B PI3K binds to G proteins (4): it has only one catalytic subunit (p110γ), which is expressed mainly in leukocytes (5), and two putative regulatory subunits (p101 and p87PIKAP) (5–7).

T cells are activated after TCR ligation. Tyr kinases are the most proximal mediators in TCR signaling: lymphocyte-specific Tyr kinase (Lck) phosphorylates Tyr residues in the immunoreceptor Tyr-based activation motifs (ITAMs) present in each of the TCR-associated CD3 chains. Once phosphorylated, the ITAMs act as docking sites, recruiting ζ-associated protein (ZAP70) to the activated TCR near activated Lck, which then phosphorylates and activates ZAP70. ZAP70 in turn phosphorylates the adaptor molecules Src homology 2 (SH2) domain–containing leukocyte protein of 76 kD and linker for activation of T cells. The linker for activation of T cells and SH2 domain–containing leukocyte protein of 76 kD signaling complexes activate the guanine nucleotide exchange factor Vav, which then activates RAS-related C3 botulinum substrate 1 (Rac1) and actin reorganization (8). F-actin polymerization at the TCR cell–cell contact site stabilizes the interaction between the T cell and the APC (9). TCR engagement also leads to PI3K activation at the immunological synapse (IS), which induces translocation of protein kinase B (PKB) to the plasma membrane (10, 11). TCR stimulation also triggers recruitment of $G\alpha_{q/11}$-coupled chemokine receptors to the IS (12), which cooperate in T cell activation.

The online version of this article contains supplemental material.

The Journal of Experimental Medicine

T cell activation is not regulated by the TCR alone: the CD4, CD8, and CD28 coreceptors complement the TCR-induced signals. p85α, the regulatory subunit of class I_A PI3K, is recruited to the TCR complex by CD3ζ or CD28, or via TCR-interacting molecule (TRIM) (13–15). Moreover, deletion of the class I_A isoform p110δ as well as p85α defects interferes with T cell activation, particularly in the $CD4^+$ T cell compartment (16, 17). p110γ deficiency also results in T cell activation defects (18, 19). Nonetheless, it is currently not known whether the TCR activates p110γ, nor by what mechanism it might do so.

In this paper, we report p110γ activation by TCR cross-linking. p110γ interacts with $G\alpha_{q/11}$, Lck, and ZAP70, and by modulating Rac1 activity, regulates F-actin polymerization. As a consequence, p110γ affects the interaction between T cells and APCs, and regulates T cell activation.

RESULTS

Reduced in vitro proliferation and expansion of p110γ-deficient T cells

p110γ-deficient T cells have a diminished anti-CD3 proliferative response, which is partially rescued by CD28 costimulation; this defect has been linked to suboptimal IL-2 production (18). We tested whether addition of exogenous IL-2 augmented TCR-induced proliferation in $p110\gamma^{-/-}$ T cells. Addition of 20 U/ml IL-2 increased CD3- and CD3/CD28-induced proliferation in $p110\gamma^{-/-}$ and $p110\gamma^{+/-}$ T cells but did not completely rescue the $p110\gamma^{-/-}$ proliferation defect (Fig. 1 A). Expansion of purified $p110\gamma^{-/-}$ T cells after TCR-induced stimulation was impaired during long time periods after stimulation, even in the presence of exogenous IL-2 (Fig. 1 B). Impaired TCR-induced proliferation in $p110\gamma^{-/-}$ T cells must therefore be caused not only by reduced IL-2 levels but also by other TCR-linked defects. Reduction of TCR-induced proliferation was similar in purified $CD4^+$ (Fig. 1 C) and $CD8^+$ (Fig. 1 D) T cells.

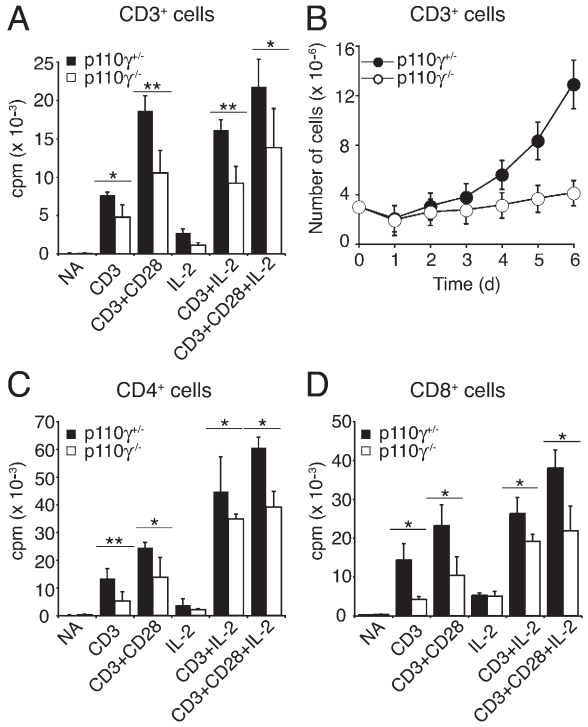

Figure 1. Impaired in vitro proliferation of $p110\gamma^{-/-}$ T cells. (A) Peripheral T cells ($CD3^+$) were purified from $p110\gamma^{-/-}$ and $p110\gamma^{+/-}$ mice and activated in wells coated with anti-CD3 or anti-CD3 plus anti-CD28, alone or with 10 U/ml IL-2. Proliferation was determined at 48 h. Means ± SD are shown for at least three experiments. *, $P \leq 0.05$; **, $P \leq 0.01$. (B) For long-term in vitro expansion, $p110\gamma^{-/-}$ and $p110\gamma^{+/-}$ peripheral T cells were activated in anti-CD3–coated wells (day 0) for 24 h; at day 1, cells were removed from antibody and 10 U/ml IL-2 was added. The total cell number was counted daily. Means ± SD are shown for three experiments ($P \leq 0.01$). (C and D) Proliferation of purified $CD4^+$ (C) or $CD8^+$ (D) T cells from $p110\gamma^{-/-}$ and $p110\gamma^{+/-}$ mice, as in A. *, $P \leq 0.05$; **, $P \leq 0.01$. NA, not activated.

p110γ is activated by TCR engagement

To determine whether p110γ is activated by the TCR, we measured p110γ lipid kinase activity after TCR complex cross-linking in purified WT $CD3^+$, $CD4^+$, and $CD8^+$ mouse T cells. $CD3^+$ cells showed transient induction of p110γ activity, with two peaks at 1–3.5 min and at 15–30 min after activation (with anti-CD3 plus anti-CD28 antibody; Fig. 2 A). We found a similar two-peak p110γ induction profile in $CD4^+$ T cells, whereas a slower and more maintained single p110γ activity peak was detected in $CD8^+$ cells (Fig. 2 B). The two-peak profile was also observed using Jurkat $CD4^+$ T cells (not depicted).

We also purified $p110\gamma^{-/-}$ and $p110\gamma^{+/-}$ mouse spleen T cells, activated them using anti-CD3 antibody, and isolated CD3- or Tyr kinase–associated proteins by immunoprecipitation. CD3-associated PI3K lipid kinase activity, which includes class I_A isoforms (13), was similar in $p110\gamma^{+/-}$ and $p110\gamma^{-/-}$ T cells, with a reduction only at late time points (Fig. 2 C). Phospho-Tyr–associated PI3K lipid kinase activity was nonetheless reduced in $p110\gamma^{-/-}$ compared with $p110\gamma^{+/-}$ T cells at all times tested (Fig. 2 C). TCR cross-linking thus activates p110γ, which associates with Tyr kinases.

Inactive p110γ prevents PIP_3 accumulation at the IS

PIP_3 concentrates at the T cell–APC IS during T cell activation (10, 11). We examined whether p110γ was concentrated at the IS after TCR stimulation, which could contribute to PIP_3 production. We transiently transfected Jurkat T cells with p110γ-GFP (Fig. 3 A, unstimulated). After incubation of cells with anti-CD3– plus anti-CD28–coated beads, p110γ-GFP localized in the cytosol near the bead contact area but did not concentrate at the IS (Fig. 3 A). It was thus possible that TCR stimulation affected p110γ activation but not p110γ localization.

To determine whether p110γ contributes to PIP_3 production at the IS, we transfected Jurkat T cells with a 3′-polyphosphoinositide–specific probe composed of the PKB-PH domain fused to GFP (GFP–PKB-PH), which binds PIP_3 and PIP_2 with

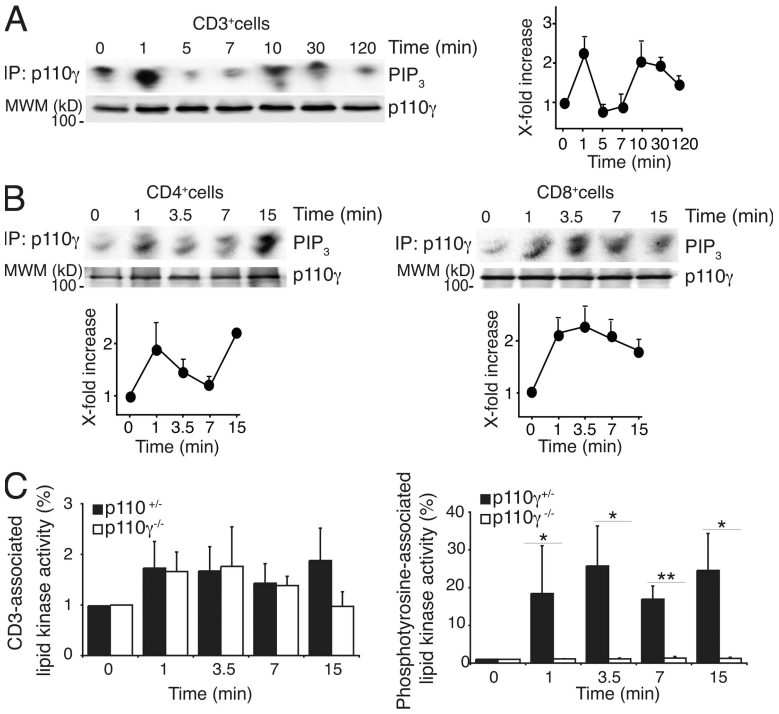

Figure 2. p110γ is activated by TCR engagement. (A) Purified T cells from WT mice were activated with anti-CD3 plus anti-CD28 for different times. p110γ was immunoprecipitated from total cell lysate, and its lipid kinase activity was determined in vitro. Lipids were resolved by TLC and visualized by autoradiography. Anti-p110γ was used in Western blots to control equal amounts of p110γ in the different extracts. The histogram represents the x-fold increase (means ± SD) of the PIP_3 signal (quantitated using ImageJ) at different time points (t) compared with that obtained at t = 0. (B) Lipid kinase activity as in A was determined in purified $CD4^+$ and $CD8^+$ T cells from WT mice (means ± SD). (C) Purified T cells from $p110\gamma^{-/-}$ and $p110\gamma^{+/-}$ spleens were activated using anti-CD3 for different times, and the CD3- or Tyr kinase–associated protein fractions were immunoprecipitated. CD3- and Tyr kinase–associated PI3K lipid kinase activity was determined by ELISA. Means ± SD are shown for three different experiments. *, $P \leq 0.05$; **, $P \leq 0.01$.

similar affinity. We used the membrane-linked GFP-$G_{\beta 1}$ plus $G_{\gamma 2}$ proteins as a specificity control. In Jurkat T cells, which lack phosphatase and tensin homologue and SH2 domain–containing inositol phosphatase expression, GFP–PKB-PH is found at the cell membrane (Fig. 3 B, top, unstimulated) (20). Incubation with anti-CD3– plus anti-CD28–coated beads nonetheless induced GFP–PKB-PH redistribution to the IS (Fig. 3 B, top, stimulated), confirming previous reports (10, 11). This redistribution was specific, as we found no GFP-$G_{\beta 1}$ redistribution after contact with anti-CD3– plus anti-CD28–coated beads (Fig. 3 B, bottom).

To determine the potential contribution of p110γ to PIP_3 relocalization at the IS, we cotransfected Jurkat T cells with GFP–PKB-PH and either p110γ WT or an inactive form of p110γ (p110γ–KR). Cell incubation with anti-CD3– plus anti-CD28–coated beads induced GFP–PKB-PH redistribution to the IS in WT p110γ-expressing cells (Fig. 3 C, bottom), but not in those bearing the inactive p110γ–KR form (Fig. 3 C, top). This suggests a role for p110γ in PIP_3 localization at the IS.

p110γ associates to Lck and ZAP70 after TCR engagement

Ligand binding to CXC chemokine receptor (CXCR) 4 induces its association with the TCR, followed by ZAP70 activation (21). Conversely, TCR stimulation induces $G\alpha_{q/11}$–coupled chemokine receptor recruitment to the IS (12). p110γ binds to $G\alpha_{q/11}$ and is activated by $G\alpha_{q/11}$ (4) after TCR cross-linking in complex with Tyr-phosphorylated proteins (Fig. 2).

We analyzed whether TCR stimulation induced p110γ association to $G\alpha_{q/11}$ or to Tyr kinases (Lck and ZAP70). We activated CXCR4-transfected Jurkat T cells by TCR cross-linking, using anti-CD3 antibodies for various time periods. To determine p110γ association, we immunoprecipitated Lck, ZAP70, and $G\alpha_{q/11}$ and examined associated p110γ in Western blots. TCR stimulation induced p110γ association in all cases: maximum complexed protein was observed for ZAP70 and $G\alpha_{q/11}$ at 1–3.5 min and for Lck at 15 min after stimulation (Fig. 4 A). We tested for the presence of p110γ, $G\alpha_{q/11}$, and Lck in complex with ZAP70. Immunoprecipitation of p110γ, $G\alpha_{q/11}$, and Lck showed transient ZAP70 association, with maximum complex formation at 1–3.5 min for p110γ and $G\alpha_{q/11}$; maximum Lck association to ZAP70 was found at 15 min after stimulation (Fig. 4 A). To define whether this complex involves chemokine receptors, we immunoprecipitated CXCR4 and examined associated proteins in Western blots. CXCR4 association with p110γ was sustained, as in a previous report (5). TCR activation moderately enhanced CXCR4 association to $G\alpha_{q/11}$ and induced a remarkable association to ZAP70 at 15 min (Fig. 4 B), confirming previous observations (12, 21).

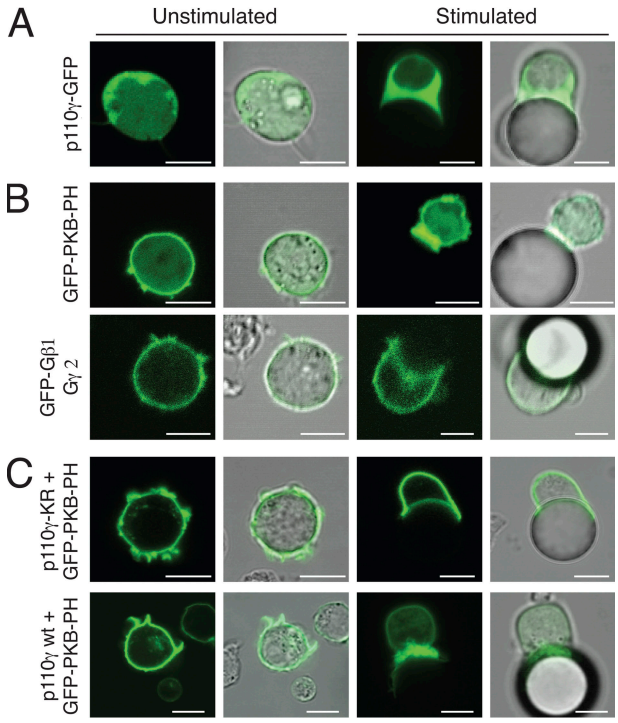

Figure 3. p110γ regulates PIP_3 accumulation at the IS. Jurkat T cells were transfected with p110γ-GFP (A), GFP–PKB-PH (B, top), or GFP-$G\beta_1$ plus $G\gamma_2$ (B, bottom), and with a combination of GFP–PKB-PH and either p110γ-KR (C, top) or p110γ-WT (C, bottom). GFP distribution was examined by confocal microscopy of live cells. (A) p110γ-GFP localized to the cell–cell contact site but did not concentrate at the IS. (B) GFP–PKB-PH is located at the cell membrane and redistributes to the IS after stimulation with anti-CD3– plus anti-CD28–coated latex beads (top). As a control, GFP-$G\beta_1$ concentrated at the IS after stimulation (bottom). (C) The PIP_3 probe GFP–PKB-PH concentrated at the IS in activated cells expressing p110γ WT (bottom) but not in cells expressing a dominant-negative p110γ form (p110γ-KR; top). For each experiment, we analyzed 100 cells. The p110γ-GFP image is representative of 80% of the cells. The GFP–PKB-PH concentration at the IS after stimulation was observed in 77% of the cells, whereas the GFP-$G\beta_1$ image represents >95% of the cells. The p110γ-KR plus GFP–PKB-PH image represents 75% of the cells, and 82% of the cells for p110γ WT plus GFP–PKB-PH. Bars: 7.5 μm.

These results suggested that T cell stimulation provokes rapid formation (1–3.5 min) of a complex that includes p110γ, $G\alpha_{q/11}$, and ZAP70 (Fig. 1 A, histogram), which would correlate with the first p110γ activation peak. This first p110γ activation peak after TCR ligation appears independent of CXCR4, which associates p110γ in a constitutive fashion and to ZAP70 only at 15 min. The complex induced by the TCR at 15 min involved ZAP70, Lck, CXCR4, and p110γ, and its formation correlated with the second p110γ activity peak.

We analyzed whether a similar complex is formed in primary T cells after TCR cross-linking. We found that p110γ associated with Lck, ZAP70, and $G\alpha_{q/11}$ in purified mouse $CD3^+$, $CD4^+$, and $CD8^+$ T cells (Fig. 4, C–E). In primary T cells, association of p110γ to Lck, Zap70, and $G\alpha_{q/11}$ occurred at early time points (1–3.5 min) after stimulation and was more persistent than in Jurkat cells, especially in $CD8^+$ T cells, in which the complexes declined slowly. These results show that TCR stimulation provokes in $CD4^+$ primary T cells rapid formation (1–3.5 min) of a complex that includes p110γ, $G\alpha_{q/11}$ Lck, and ZAP70, which would correlate with the first p110γ activation peak observed in these cells and in whole $CD3^+$ populations (Fig. 2). In $CD8^+$ T cells, the complex induced by TCR ligation appeared and declined more slowly, correlating with p110γ activation in these cells. In addition, in $CD3^+$ and $CD4^+$ T cells, $G\alpha_{q/11}$ association to p110γ (Fig. 4, C and D) and to Zap 70 (not depicted) increased again at 15 min. This observation reflects formation of a complex including p110γ, $G\alpha_{q/11}$, and Zap 70; this complex may include chemokine receptors, as observed in Jurkat cells (Fig. 4, A and B) and in previous studies (12). Formation of this complex correlates with the second p110γ activity peak induced by T cell activation (Fig. 2).

T cell signaling downstream of the TCR is impaired in p110γ$^{-/-}$ mice

To determine whether p110γ contributes to TCR-activated signaling cascades, we compared activation of Tyr, PKB, and mitogen-activated protein kinase (MAPK) in highly purified p110γ$^{+/-}$ and p110γ$^{-/-}$ T cells stimulated with anti-CD3 alone or with anti-CD28 mAb. Anti–phospho-Tyr Western blots of p110γ$^{-/-}$ and p110γ$^{+/-}$ T cell extracts showed several protein bands (25–75 kD) with reduced Tyr phosphorylation after CD3 stimulation alone or with CD28 (Fig. 5 A). Similarly, although the anti–phospho-PKB signal was substantially increased in p110γ$^{+/-}$ T cells, activation was lower in p110γ$^{-/-}$ T cells (Fig. 5 B). Anti–phospho-p44/42 MAPK analysis showed increased p44/42 MAPK phosphorylation in p110γ$^{+/-}$ T cells after TCR stimulation alone or with anti-CD28; this was significantly impaired in p110γ$^{-/-}$ T cells (Fig. 5 C), concurring with p110γ involvement in MAPK activity (22). Purified $CD4^+$ and $CD8^+$ T cells gave consistent results in Western blot analyses (unpublished data). The data indicate a broad effect of p110γ deletion on TCR downstream signals, including activation of Tyr kinases, PKB, and MAPK.

Impaired Rac activity in p110γ-deficient mice

This overall defect in TCR-induced signaling pathways in the absence of p110γ led us to test whether p110γ has a role in IS formation and/or maintenance. Because PI3K regulates Rac activity (23), Rac regulates actin polymerization, and polymerized actin is required for synapse stability (24), we postulated that p110γ could contribute to T cell activation by regulating Rac activity and, thus, actin polymerization.

Purified T cells from p110γ$^{+/-}$ and p110γ$^{-/-}$ mice were rested in serum-free medium to reduce basal Rac activation levels, then activated by TCR cross-linking for varying periods. Cells were lysed in GST-FISH buffer, and total protein lysate was tested in a Rac pulldown assays (25). We observed a lower and delayed induction of Rac activity in p110γ$^{-/-}$ than in p110γ$^{+/-}$ $CD3^+$ cells after TCR ligation (Fig. 6 A).

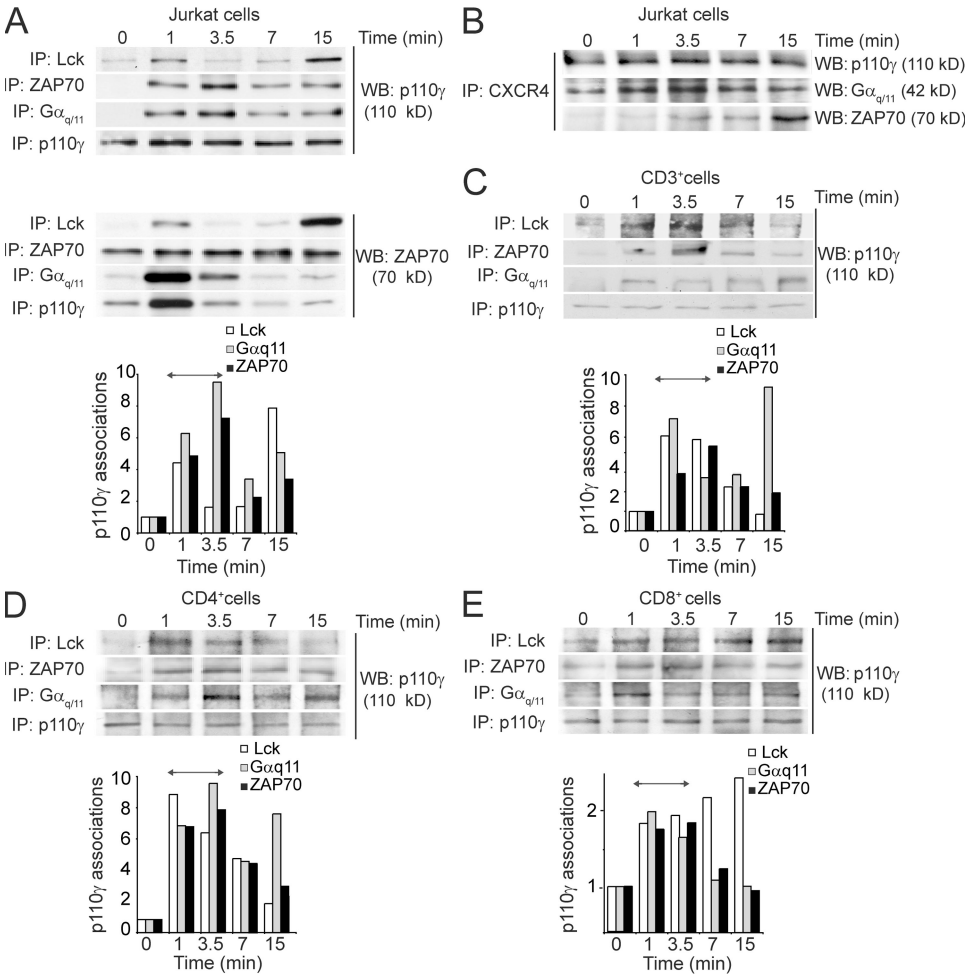

Figure 4. p110γ interacts with Lck and ZAP70, and is downstream of CD3. Jurkat T cells were transiently transfected with pEGFP-CXCR4. After 36 h, cells were collected and activated with anti-CD3 mAb for different times. Lysates were immunoprecipitated using anti-Lck, -ZAP70, -$G\alpha_{q/11}$, or -p110γ mAb and blotted with anti-p110γ (A, top) and anti-ZAP70 (A, bottom) mAb. (B) Lysates were immunoprecipitated with anti-GFP (CXCR4) and blotted with anti-p110γ, $G\alpha_{q/11}$, or ZAP70. (C) Purified T cells ($CD3^+$), (D) purified $CD4^+$ T cells, or (E) purified $CD8^+$ T cells from WT mice were collected and activated with anti-CD3 mAb for different times. Lysates were immunoprecipitated using anti-Lck, -ZAP70, -$G\alpha_{q/11}$, or -p110γ mAb and blotted with anti-p110γ mAb. The histograms represent the x-fold increase in the Western blot signal of p110γ associated to Lck, ZAP70, or $G\alpha_{q/11}$ at different time points (t), quantitated using ImageJ and compared with that obtained at t = 0. Arrows indicate maximum complex formation.

This defective activation was partially compensated at early time points by simultaneous anti-CD3 plus anti-CD28 cross-linking, but late Rac activation was still defective (Fig. 6 A). Using purified anti-CD3–activated $CD4^+$ and $CD8^+$ T cells, we confirmed the lower TCR induction of Rac activation in both populations from $p110\gamma^{-/-}$ mice (Fig. 6, B and C); the defect was more remarkable at late time points. In most experiments, basal Rac activity levels (time 0) were slightly higher in $p110\gamma^{-/-}$ compared with $p110\gamma^{+/-}$ T cells, whereas Western blot analysis showed similar Rac protein levels (Fig. 6, A–C). Analysis of the expression of p110 isoforms showed a moderately higher p110β expression in $p110\gamma^{-/-}$ than in $p110\gamma^{+/-}$ T cells, which could explain the higher background levels in $p110\gamma^{-/-}$ (Fig. 6 D). Despite higher basal activity, TCR-triggered Rac activation was defective in $p110\gamma^{-/-}$ T cells, showing that p110γ controls Rac activation by the TCR.

$p110\gamma^{-/-}$ T cells show decreased TCR-induced actin polymerization

TCR-induced T cell activation causes reorganization of the actin cytoskeleton, resulting in F-actin polymerization at the T cell–APC contact site. As Rac controls actin polymerization, we studied potential actin polymerization defects in $p110\gamma^{-/-}$ mice. We examined F-actin levels after CD3 cross-linking, using GFP-phalloidin to stain F-actin in permeabilized $p110\gamma^{-/-}$ and $p110\gamma^{+/-}$ T cells. F-actin levels were similar in unstimulated $p110\gamma^{-/-}$ and $p110\gamma^{+/-}$ $CD4^+$ T cells (unpublished data). Nonetheless, after TCR stimulation, $p110\gamma^{+/-}$ mouse $CD4^+$ T cells showed increased F-actin and a less pronounced, less sustained increase in $p110\gamma^{-/-}$ mice. Co-stimulation with anti-CD28 did not rescue this defect in $CD4^+$ T cells (Fig. 7 A). Similar defects were observed in $p110\gamma^{-/-}$ $CD8^+$ T cells (Fig. 7 B).

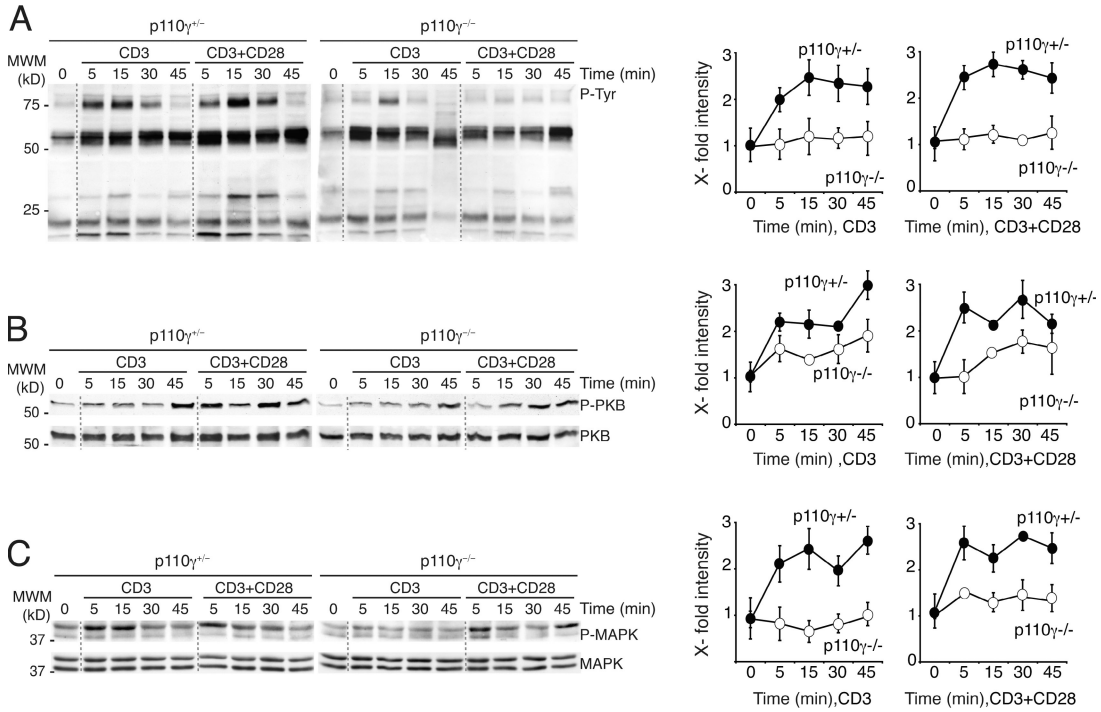

Figure 5. Impaired signaling downstream of TCR in p110γ$^{-/-}$ mice. Purified peripheral T cells from p110γ$^{-/-}$ and p110γ$^{+/-}$ mice were stimulated by cross-linking with anti-CD3 or anti-CD3 plus anti-CD28 for the times indicated. T cell lysates were resolved in SDS-PAGE, followed by Western blot with (A) anti–phospho-Tyr (P-Tyr), (B) anti–phospho-PKB (P-PKB) and anti-PKB, and (C) anti–phospho-p44/42 MAPK (P-MAPK) and anti-p44/42 MAPK (MAPK) antibodies; anti-PKB and -MAPK antibodies were used as loading controls, as indicated. The figures show one representative blot of at least three experiments with similar results. Data from the Western blots were quantified by densitometry using ImageJ software and are reported as the x-fold intensity increase compared with t = 0. Dashed lines separate blots for different activation conditions. Histograms represent means ± SD of three (P-PKB and P-ERK) or four (P-Tyr) experiments with similar results (A, $P \leq 0.01$; B, $P \leq 0.05$; C, $P \leq 0.01$). In the P-Tyr blot, numbers indicate molecular weight markers (MWM; left).

We also examined whether interference with endogenous p110γ activity in Jurkat cells affected actin polymerization after TCR-induced stimulation. Jurkat cells transfected with empty vector, p110γ WT, or the inactive p110γ-KR were stimulated with anti-CD3 alone or anti-CD3 plus anti-CD28 mAb, and FITC-phalloidin staining was measured by flow cytometry at various times. Control cells showed increased F-actin polymerization in both TCR activation protocols, which was enhanced by p110γ WT and inhibited by p110γ-KR overexpression (Fig. 7 C). These results indicate a key role for p110γ in TCR-induced actin polymerization.

T cell–APC conjugate formation is impaired in p110γ$^{-/-}$

F-actin polymerization at the TCR cell–cell contact site stabilizes the interaction between the T cell and the APC (9). To study p110γ involvement in the maintenance of T cell–APC conjugates, we purified primary CD4$^+$ T cells from 5CC7 transgenic (Tg) × p110γ$^{-/-}$ and 5CC7 Tg × p110γ$^{+/-}$ mice. The 5CC7 TCR recognizes pigeon cytochrome c (PCC) peptide$_{88–104}$ in the MHC class II I-E^k context. For APCs, we purified splenic B cells from 5CC7 Tg × p110γ$^{+/-}$ mice. Using a FACS-based assay, we measured the ability of p110γ$^{-/-}$ and p110γ$^{+/-}$ T cells to form conjugates with peptide-pulsed B cells (26); B cells were labeled with the green dye PKH67, and T cells were labeled with the red dye PKH26. In the absence of peptide, we observed no 5CC7 Tg CD4$^+$ T cell conjugates. After peptide-induced TCR stimulation, the percentage of 5CC7 Tg × p110γ$^{+/-}$ CD4$^+$ cell conjugates was twofold higher than in the same cell subset from p110γ$^{-/-}$ littermates (Fig. 8 A). These data illustrate that a weaker T cell–APC interaction occurs in p110γ$^{-/-}$ compared with p110γ$^{+/-}$ T cells.

To confirm these observations and extend them to CD8$^+$ T cells, we purified CD8$^+$ T cells from F5 Tg × p110γ$^{-/-}$ and F5 Tg × p110γ$^{+/-}$ mice and incubated them with B cells from F5 Tg × p110γ$^{+/-}$ mice. The TCR expressed on F5TCR Tg specifically recognizes the influenza peptide NP$_{366–374}$ in the MHC class I H-2D^b context. After addition of the specific peptide, the percentage of F5 Tg × p110γ$^{+/-}$ CD8$^+$ cell conjugates was twofold higher than in the same subset from p110γ$^{-/-}$ littermates (Fig. 8 B), confirming the role of p110γ in T cell–APC conjugate stabilization.

Based on these observations, we predicted that interference with endogenous p110γ activity in T cells would inhibit cell conjugate formation. We transfected Jurkat T cells with empty vector, p110γ WT, or p110γ–KR. At 48 h after transfection, the cells were tested in a conjugate formation assay

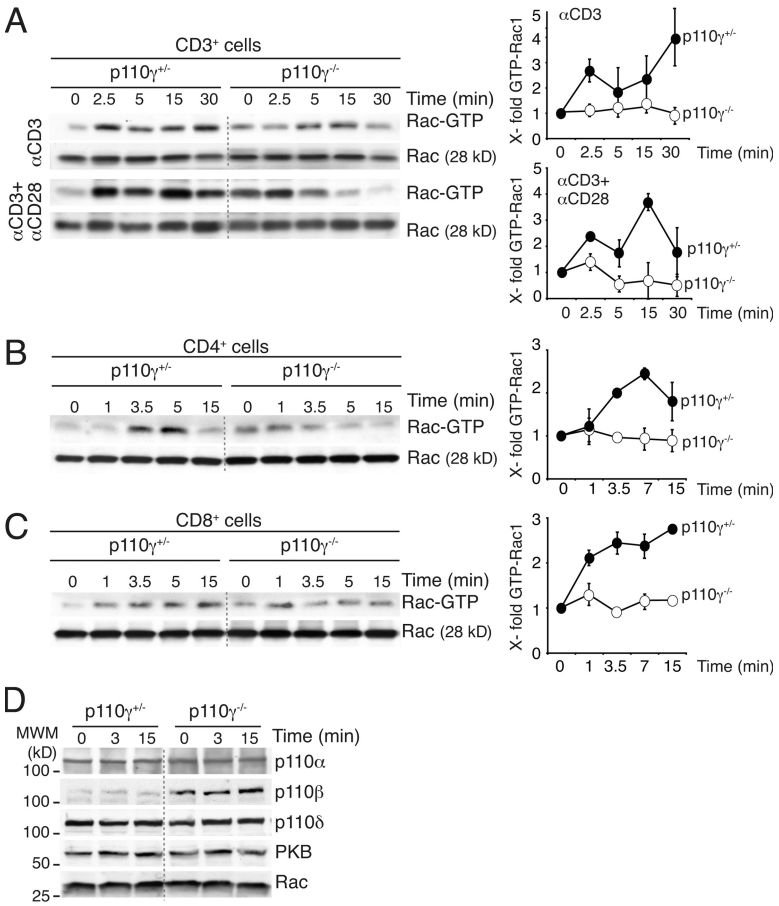

Figure 6. p110γ controls Rac activation downstream of the TCR. (A) Rac activity assay in purified p110γ$^{-/-}$ and p110γ$^{+/-}$ peripheral T cells. T cells were stimulated with soluble anti-CD3 antibody or anti-CD3 plus anti-CD28 antibody. Extracts were analyzed in pulldown assays using Gex2T-CRIB^{Pak1} as bait. Rac-GTP and total Rac cell content were examined by Western blotting. One representative analysis is shown out of three performed. Data from Western blots were quantified by densitometry and are reported as the x-fold intensity of the GTP-Rac1 signal compared with that observed at t = 0. Data represent means ± SD of three experiments. (B) Rac activity assay in purified CD4$^+$ p110γ$^{-/-}$ and p110γ$^{+/-}$ T cells as in A. (C) Rac activity assay in purified CD8$^+$ p110γ$^{-/-}$ and p110γ$^{+/-}$ T cells as in A. (D) Representative immunoblots of class I_A p110α, p110β, and p110δ subunits in purified p110γ$^{-/-}$ and p110γ$^{+/-}$ CD3$^+$ peripheral T cells. PKB and Rac Western blots illustrate equal loading. Dashed lines separate blots for different mouse phenotypes. MWM, molecular weight markers.

using staphylococcal enterotoxin E (SEE)–loaded Raji cells. Although p110γ WT enhanced conjugate formation, the proportion of conjugates was reduced in p110γ-KR–transfected Jurkat cells (Fig. 8 C). These observations show that p110γ regulates conjugate formation between T cells and APC.

DISCUSSION

Mice lacking p110γ have a partial defect in T cell differentiation and activation. We sought to determine how the TCR regulates p110γ activity in T cells. In this study, we show that p110γ is activated by the TCR, which induces association of p110γ with $G\alpha_{q/11}$, and with the ZAP70 and Lck Tyr kinases. p110γ regulates Rac activation and in turn F-actin polarization, which stabilizes conjugate formation between T cells and APCs.

p110γ has a central role in neutrophil and macrophage migration to inflammatory sites (18). Despite p110γ regulation of thymocyte exit to the periphery (19), however, this enzyme is less important for chemokine-induced T cell migration (unpublished data) (27). p110γ might nonetheless have other functions in immunocompetent T cells, because T cells lacking p110γ have defects in TCR-induced cell activation (18). Moreover, in addition to class I_A involvement in T cell activation (16), class I_B PI3K controls TCR- and pre-TCR–induced T cell differentiation (19) as well as memory T cell generation (28, 29). p110γ might thus collaborate with class I_A PI3K to activate T cells. The partial maintenance of T cell function in the absence of class I_A PI3K (30) and the remarkable thymocyte differentiation defect in both class I_A p110δ- and class I_B p110γ-deficient mice (31, 32) indicate a role for p110γ in TCR-induced T cell activation. These results imply an important function for p110γ in TCR-mediated T cell activation.

We show that p110γ is activated by TCR ligation. p110γ was known to be activated in response to GPCR by direct binding to G protein βγ subunits (4, 33), whereas the link between p110γ and the TCR was less clear. Class I_A PI3K p85α binds the TCR CD3ζ chain and to the CD28 coreceptor (13, 14);

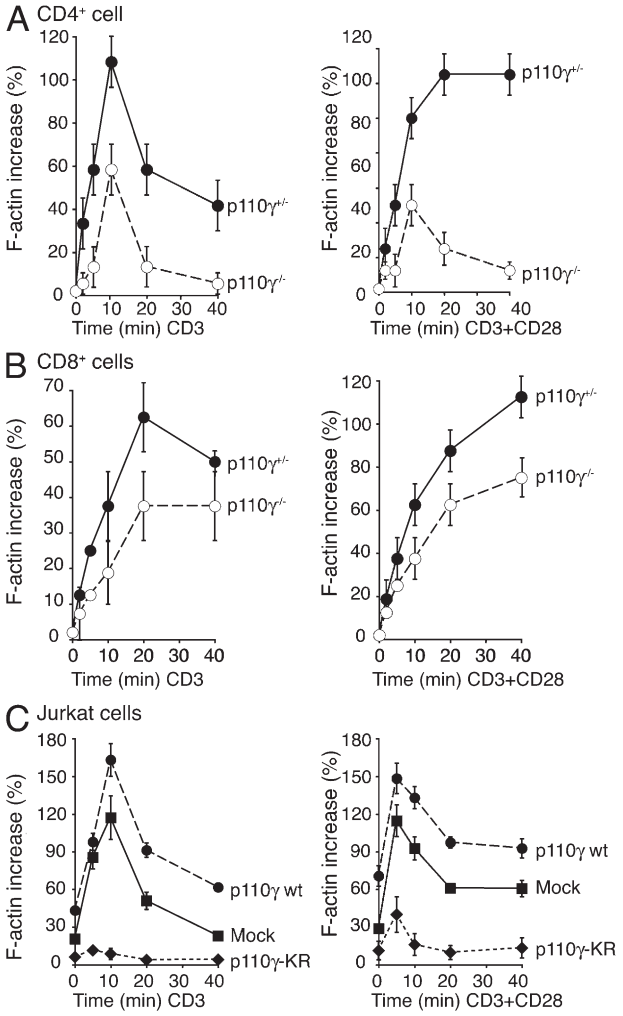

Figure 7. p110γ regulates TCR-induced actin polymerization. (A and B) CD4+ (A) or CD8+ (B) purified T cells from p110γ$^{-/-}$ and p110γ$^{+/-}$ mice were stimulated with soluble anti-CD3 or anti-CD3 plus anti-CD28 mAb for the times indicated. Phalloidin staining was determined by flow cytometry and is expressed as the increase in mean fluorescence intensity over that observed at t = 0. Means ± SD are shown for three independent experiments. (C) p110γ interferes with actin polymerization in Jurkat T cells. Jurkat T cells were transfected with vector alone, p110γ, or p110γ-KR (48 h) and activated with soluble anti-CD3 or anti-CD3 plus anti-CD28 mAb for the times indicated. Phalloidin staining was determined by flow cytometry and is expressed as in A. Means ± SD are shown for three independent experiments.

PI3K activity is also associated with CD3ε after TCR engagement (34). We show that class I_B p110γ is downstream of TCR signaling, and that TCR cross-linking with anti-CD3 antibodies activates p110γ and induces its association with Lck, ZAP70, and $G\alpha_{q/11}$. This association may be direct or mediated via an intermediate adaptor. During T cell stimulation by APCs, chemokine receptors couple to $G\alpha_{q/11}$ proteins, which are recruited to the IS on T cells; chemokine receptor trapping at the synapse enhances T cell activation (12). The CXC chemokine ligand 12 stimulates physical association of CXCR4 and the TCR, and uses the TCR ITAM domains and ZAP70 for signal transduction (21). Another study showed physical association between CD3ε and $G\alpha_{q/11}$, and that CD3 ligation induces GTP exchange within $G\alpha_{q/11}$ (35); this suggested that after TCR engagement, $G\alpha_{q/11}$ participates in pathways that mediate CD3 Tyr phosphorylation. Our results indicate that TCR stimulation induces p110γ association to $G\alpha_{q/11}$, ZAP70, and Lck, all of which are critically involved in TCR activation. In CXCR4-transfected Jurkat T cells, p110γ activation shows two peaks, the first of which correlates with p110γ association with $G\alpha_{q/11}$, Lck, and ZAP70 but not with increased CXCR4 association to p110γ or ZAP70. The second peak correlates with enhanced p110γ association with Lck, ZAP70, and CXCR4. p110γ activation is thus initially CXCR4 independent and is linked to the direct p110γ association with $G\alpha_{q/11}$ and Tyr kinases. Formation of the p110γ–$G\alpha_{q/11}$–Lck–ZAP70 complex could bring p110γ into proximity with the IS, enhancing local PIP_3 production. Similar complexes could also enhance PIP_3 production at the IS in CD4+ and CD8+ peripheral T cells, because the complex formation is faster but less sustained in CD4+ than in CD8+ T cells.

APC activation of T cells begins with formation of the IS, a highly organized complex of surface receptors, intracellular signaling molecules, and F-actin at the T cell contact site (36, 37). TCR cross-linking enhances PIP_3 production, which concentrates at the IS in T cells; PI3K activation then induces PKB translocation to the plasma membrane (10, 11). We confirm PIP_3 accumulation at the T cell contact site with the APC; p110γ did not localize exclusively to the IS, but was activated within the synapse when it complexed with CD3-associated Tyr kinases. GFP–PKB-PH localization experiments showed that expression of a dominant-negative p110γ reduced PIP_3 concentration at the synapse. These results indicate that p110γ activity regulates PIP_3 content at the IS.

Actin cytoskeleton rearrangement is critical at several points in TCR-induced cell activation (9, 37), including IS formation and maintenance (38–40). Studies in a variety of cell types identify Rac as a key modulator of F-actin polymerization (41). Cytoskeletal reorganization by GPCR depends on p110γ as well as on Rac (42). p110γ participates in Rac1 activation after CC chemokine ligand 5 stimulation of macrophages (43). Rac also controls actin polymerization in both CD4+ and CD8+ T cells (39, 44). TCR ligation activates p110γ, which in turn regulates Rac activity, because interference with p110γ reduced and delayed Rac activation. These Rac activation defects explain the reduced F-actin levels in p110γ$^{-/-}$ T cells compared with controls after TCR cross-linking. In addition, actin did not polymerize in PI3Kγ-KR–transfected Jurkat cells. Our results thus demonstrate a critical role for p110γ in TCR-induced, Rac-mediated actin polymerization.

p110γ$^{-/-}$ CD4+ and CD8+ T cells also showed reduced T cell–APC conjugate formation, suggesting that T cell–APC interaction is weaker in p110γ$^{-/-}$ than in p110γ$^{+/-}$ T cells. Accordingly, the proportion of T cell–APC conjugates was clearly reduced in PI3Kγ-KR–transfected Jurkat cells,

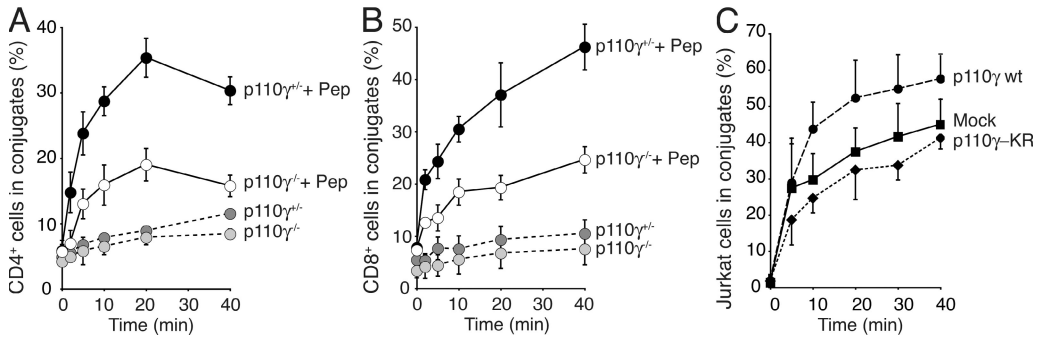

Figure 8. p110γ regulates cell conjugate formation. (A) p110γ$^{-/-}$ CD4+ T cells showed impaired TCR-induced conjugate formation. Purified CD4+ T cells were obtained from 5CC7 Tg × p110γ$^{-/-}$ and 5CC7 Tg × p110γ$^{+/-}$ spleens. For APCs, B cells were purified from 5CC7 Tg × p110γ$^{+/-}$ spleens. T cells were labeled with PKH67 (green) and APCs were labeled with PKH26 (red), and B cells were pulsed with PCC peptide$_{88-104}$. Conjugate formation, as determined by flow cytometry, is represented as the T cell fraction that shifted into two-color conjugates. Means ± SD are shown for three independent experiments. (B) TCR-induced conjugate formation was impaired in p110γ$^{-/-}$ CD8+ T cells. Purified CD8+ T cells were obtained from F5 Tg × p110γ$^{-/-}$ and F5 Tg × p110γ$^{+/-}$ spleens; B cells (APCs) were purified from F5 Tg × p110γ$^{+/-}$ spleens. Cells were labeled as in A, and B cells were pulsed with the influenza peptide NP$_{366-374}$. Conjugate formation was determined as in A. (C) p110γ interferes with conjugate formation in Jurkat T cells. Jurkat cells were transfected with vector alone, p110γ, or p110γ-KR (48 h) and mixed with SEE-loaded Raji B cells for the times indicated. Conjugate formation was determined as in A.

showing that p110γ regulates conjugate formation between T cells and APCs.

Most of the defects described in this paper affect p110γ$^{-/-}$ CD4+ and CD8+ T cells similarly. This is not surprising, as p110γ formed a similar complex in both CD4+ and CD8+ cells after TCR activation (Fig. 4). Nonetheless, induction of p110γ complexes in WT CD8+ T cells was slower, probably reflecting a lesser CD8+ T cell dependence on p110γ for early T cell activation. In accordance with these observations, we found a less pronounced defect in TCR activation-induced actin polymerization in p110γ$^{-/-}$ CD8+ than in CD4+ cells. Despite a requirement for Vav1 in both lineages, a point mutation in the Vav1 PH domain selectively affects TCR-induced proliferation of CD4+ but not CD8+ T cells, suggesting differential wiring of TCR signaling pathways in these two cell types (45), a possibility that might also be supported by our data.

In this paper, we demonstrate that p110γ is activated after TCR cross-linking and binds Gα$_{q/11}$, Lck, and ZAP70. Activated p110γ regulates Rac activation and actin polymerization, which governs the stability of the IS (9, 37, 38). We show that p110γ deletion affects the activation of many downstream pathways after TCR cross-linking, as well as the interaction between T cells and APCs, which could explain the defective activation of p110γ$^{-/-}$ T cells. Collectively these observations clarify the p110γ activation mechanism and mode of action in the control of T cell activation.

MATERIALS AND METHODS

Mice. p110γ$^{-/-}$ mice were previously described (46) and were maintained in heterozygosis. 5CC7 TCR (Vβ3Vα11) and F5 TCR (Vβ11Vα4) Tg mice (47, 48) were provided by M. Davis (Howard Hughes Medical Institute, Stanford, CA) and D. Kioussis (Medical Research Council, London, UK), respectively. F5TCR Tg mice were crossed with p110γ$^{-/-}$ mice; 5CC7 TCR Tg mice were crossed with p110γ$^{-/-}$ mice on the C57BL/6 background (a gift from Serono International, Geneva, Switzerland). Offspring were analyzed by PCR and flow cytometry to confirm TCR and MHC. Mice were bred and maintained in specific pathogen-free conditions in our animal facility; all animal studies were approved by the Ethics Committee for Animal Experimentation at the CNB in compliance with European Union legislation.

Primary cells. Spleen and lymph node cell suspensions were T cell enriched by depletion of B cells using mouse pan B (B220) Dynabeads (Invitrogen), followed by incubation for 2 h at 37°C on plastic plates to eliminate adherent cells, or using the CD3 negative isolation kits (Invitrogen); T cells were 90–95% CD3+ by FACS analysis (Epics XL-MCL; Beckman Coulter). For CD4+ or CD8+ cells, T cell–enriched suspensions were depleted of CD8+ or CD4+ cells using Dynabeads or using CD4 or CD8 negative isolation kits (Invitrogen). When B cells were used as APCs, T cells were depleted from suspensions with mouse pan T (Thy1.2) Dynabeads (Invitrogen). For conjugation assays, F5 Tg mouse B cells were pulsed overnight at 37°C with 2 μg/ml of influenza peptide NP$_{366-374}$, or 5CC7 Tg mouse B cells were pulsed with 2 μg/ml PCC peptide$_{88-104}$.

Cloning and expression constructs. The construct encoding the PKB-PH domain in the pEGFP-C1 vector was a gift of J. Downward (Cancer Research, London, UK). The PI3Kγ-GFP construct, a C-terminal GFP-tagged PI3Kγ, was donated by R. Wetzker (Friedrich-Schiller University, Jena, Germany). We also used p110γ WT and p110γ-KR (a dominant-negative PI3Kγ form) cloned in the pcDNA3 vector, pEGFP-CXCR4 (a gift of M. Mellado, CNB, Madrid, Spain), pCEFL EGFP Gβ1, and PCEFL Gγ2 (both gifts from J.S. Gutkind, National Institutes of Health, Bethesda, MD).

Cell lines and transfections. Jurkat T cells were maintained in DMEM (BioWhittaker) with 10% FBS (Sigma-Aldrich), 2 mM glutamine, 50 μM 2-mercaptoethanol, and 100 U/ml penicillin/streptomycin. 1.5 × 10^7 cells in 400 μl of complete medium were transfected by electroporation of 25 μg DNA using a GenePulser (270 V, 950 μF; Bio-Rad Laboratories). Cells were immediately transferred to 10 ml of growth medium and assayed 24–48 h later, when FACS or Western blot analyses showed maximum expression.

The Raji lymphoblastoid cell line was maintained in RPMI 1640 (BioWhittaker) supplemented as described in the previous paragraph. For conjugation assays, 10^7 Raji cells per milliliter were resuspended in serum-free RPMI and incubated with 1 μg/ml SEE (Toxin Technology) for 2 h at 37°C, with mixing every 20 min.

T cell activation. For biochemical analysis, immunoprecipitation assays, and actin polymerization assays, we incubated purified mouse T cells, Jurkat T cells, or Jurkat transfectants for 2 h in DMEM with 0.1% BSA (fraction V low

endotoxin; Sigma-Aldrich), after which cells were washed and resuspended in serum-free medium. For activation, 5–10 × 10^6 cells were incubated in 1.5-ml Eppendorf tubes with 1 μg/ml of soluble anti-CD3 or 1 μg/ml of anti-CD3 plus anti-CD28 for 15 min on ice, and were then cross-linked with 1 μg/ml of secondary antibody for 10 min on ice, followed by incubation at 37°C for various time periods, as shown in the figures. Cells were collected and processed for analysis. For proliferation and expansion assays, plastic wells were coated with 5 μg/ml anti-CD3 or 1.25 μg/ml anti-CD3 plus anti-CD28. Antibodies used were hamster anti–mouse CD3ε (145-2C11) and CD28 (37.51), mouse anti–human CD3ε (UCHT1) and CD28 (CD28.2), mouse anti–Armenian and –Syrian hamster IgG1 (G94-56), mouse anti–Armenian hamster IgG (G192-1; all obtained from BD Biosciences), and rabbit anti–mouse IgG (Fcγ fragment specific; Jackson ImmunoResearch Laboratories).

Proliferation and expansion assays. Plastic wells were coated as described in the previous section with anti-CD3 or anti-CD3 plus anti-CD28, and cells were added to plates, followed by 20 U/ml IL-2. After 48 h, 1 μCi [^{3}H]thymidine was added, and incorporation was measured 12 h later. Splenic T cells from p110$\gamma^{+/-}$ and p110$\gamma^{-/-}$ mice were cultured with platebound anti-CD3 for 48 h and then in flasks with 20 U/ml IL-2. Cells were counted at the times indicated in the figures.

Lipid kinase activity assays. 5–10 × 10^6 purified mouse T cells were incubated with 0.1% BSA, washed, and resuspended in serum-free medium, then activated with hamster anti-CD3 mAb and cross-linked with secondary antibodies, as described. Cells were lysed in digitonin lysis buffer (1% digitonin, 300 mM NaCl, 2 mM EDTA, 20 mM triethanolamine [pH 8], 20% glycerol, 1 μg/ml leupeptin, 1 μg/ml aprotinin, 5 mM NaF, 1 mM orthovanadate, 1 mM phenylmethanesulphonylfluoride, and 2 nM okadaic acid) and immunoprecipitated (100 μg) with 3 μl anti-CD3 or 3 μl anti–phospho-Tyr (4G10; Millipore), followed by protein A–sepharose for 1 h at 4°C. Precipitates were washed three times with 50 mM Tris-HCl, pH 7.4, and tested by ELISA to detect PI3K activity (Echelon).

Alternatively, precipitates were used as substrate for a lipid kinase reaction. To start, 20 μl PIP_2 (0.5 mg/ml in 10 mM Hepes, 0.1 mM EDTA, pH 7) and 5 μl of the phosphorylation mixture (10 mM Hepes, 0.1 mM EDTA [pH 7], 100 mM $MgCl_2$, 10 μCi [^{32}P]ATP, 200 mM ATP) were added to the pellets at room temperature for 10 min. To terminate the reaction, we added 100 μl of 1-M HCl, followed by 200 μl chloroform/methanol (1:1). The phases were separated by centrifugation, and 100 μl of the lower organic phase were washed with 80 μl methanol/HCl (1:1). Lipids were dried, resuspended in 10 μl chloroform/methanol (2:1), resolved by TLC in chloroform/methanol/NH_4OH (9:7:2), and visualized by autoradiography.

Statistical analyses. Statistical analyses were performed using StatView 512+ software (SAS Institute). Gel bands and fluorescence intensity were quantitated with ImageJ software (National Institutes of Health).

Online supplemental material. Information on Western blots, Immunoprecipitation assays, the Rac activation assay, the FACS-based conjugate formation assay, the Actin polymerization assay, and Stimulation with antibody-coated beads and immunofluorescence are available in Supplemental materials and methods. Online supplemental material is available at http://www.jem.org/cgi/content/full/jem.20070366/DC1.

We thank Drs. I. Mérida and D. Balomenos for critical reading of the manuscript and helpful suggestions, and D. Kioussis, M.M. Davis, Serono International, R. Wetzker, J. Downward, M. Mellado, and J.S. Gutkind for mice, antibodies, constructs, and vectors. We also thank C. Hernández and L. Sanz for excellent technical assistance, the CNB animal facility for aid in maintaining mouse colonies, M.C. Moreno-Ortiz for cytofluorometry studies, and C. Mark for editorial assistance.

I. Alcázar holds a predoctoral fellowship from the Association for International Cancer Research, M. Marqués receives a predoctoral fellowship from the Spanish Ministry of Education and Science University Instructor Training Program, and D.F. Barber held a Ramón y Cajal contract from the Spanish Ministry of Education and Science and a Contract-in-Aid from the Fundación Científica de la Asociación Española Contra el Cancer. This work was supported by grants from the European Union (QLRT2001-02171), the Community of Madrid (8.3/0030/2000), the Ramon Areces Foundation (to D.F. Barber and A.C. Carrera), and the Spanish Dirección General de Ciencia y Desarrollo Tecnológico (SAF2004-00815 and SAF2004-05955-C02-01 to D.F. Barber A.C. Carrera, respectively). The Department of Immunology and Oncology was founded and is supported by the Spanish National Research Council (Consejo Superior de Investigaciones Cientificas) and by Pfizer.

The authors have no conflicting financial interest.

Submitted: 20 February 2007
Accepted: 16 October 2007

REFERENCES

1. Fruman, D.A. 2004. Phosphoinositide 3-kinase and its targets in B-cell and T-cell signaling. *Curr. Opin. Immunol.* 16:314–320.
2. Okkenhaug, K., and B. Vanhaesebroeck. 2003. PI3K in lymphocyte development, differentiation and activation. *Nat. Rev. Immunol.* 3: 317–330.
3. Stephens, L.R., A. Eguinoa, H. Erdjument-Bromage, M. Lui, F. Cooke, J. Coadwell, A.S. Smrcka, M. Thelen, K. Cadwallader, P. Tempst, and P.T. Hawkins. 1997. The G beta gamma sensitivity of a PI3K is dependent upon a tightly associated adaptor, p101. *Cell.* 89:105–114.
4. Lopez-Ilasaca, M., P. Crespo, P.G. Pellici, J.S. Gutkind, and R. Wetzker. 1997. Linkage of G protein-coupled receptors to the MAPK signaling pathway through PI 3-kinase gamma. *Science.* 275:394–397.
5. Stoyanov, B., S. Volinia, T. Hanck, I. Rubio, M. Loubtchenkov, D. Malek, S. Stoyanova, B. Vanhaesebroeck, R. Dhand, B. Nürnberg, et al. 1995. Cloning and characterization of a G protein-activated human phosphoinositide-3 kinase. *Science.* 269:690–693.
6. Suire, S., J. Coadwell, G.J. Ferguson, K. Davidson, P. Hawkins, and L. Stephens. 2005. p84, a new Gbetagamma-activated regulatory subunit of the type IB phosphoinositide 3-kinase p110gamma. *Curr. Biol.* 15:566–570.
7. Voigt, P., M.B. Dorner, and M. Schaefer. 2006. Characterization of p87PIKAP, a novel regulatory subunit of phosphoinositide 3-kinase gamma that is highly expressed in heart and interacts with PDE3B. *J. Biol. Chem.* 281:9977–9986.
8. Samelson, L.E. 2002. Signal transduction mediated by the T cell antigen receptor: the role of adapter proteins. *Annu. Rev. Immunol.* 20:371–394.
9. Penninger, J.M., and G.R. Crabtree. 1999. The actin cytoskeleton and lymphocyte activation. *Cell.* 96:9–12.
10. Harriague, J., and G. Bismuth. 2002. Imaging antigen-induced PI3K activation in T cells. *Nat. Immunol.* 3:1090–1096.
11. Costello, P.S., M. Gallagher, and D.A. Cantrell. 2002. Sustained and dynamic inositol lipid metabolism inside and outside the immunological synapse. *Nat. Immunol.* 3:1082–1089.
12. Molon, B., G. Gri, M. Bettella, C. Gomez-Mouton, A. Lanzavecchia, C. Martínez-A, S. Manes, and A. Viola. 2005. T cell costimulation by chemokine receptors. *Nat. Immunol.* 6:465–471.
13. Carrera, A.C., L. Rodriguez-Borlado, C. Martinez-Alonso, and I. Merida. 1994. T cell receptor-associated alpha-phosphatidylinositol 3-kinase becomes activated by T cell receptor cross-linking and requires pp56lck. *J. Biol. Chem.* 269:19435–19440.
14. Pages, F., M. Ragueneau, R. Rottapel, A. Truneh, J. Nunes, J. Imbert, and D. Olive. 1994. Binding of phosphatidylinositol-3-OH kinase to CD28 is required for T-cell signalling. *Nature.* 369:327–329.
15. Bruyns, E., A. Marie-Cardine, H. Kirchgessner, K. Sagolla, A. Shevchenko, M. Mann, F. Autschbach, A. Bensussan, S. Meuer, and B. Schraven. 1998. T cell receptor (TCR) interacting molecule (TRIM), a novel disulfide-linked dimer associated with the TCR–CD3–ζ complex, recruits intracellular signaling proteins to the plasma membrane. *J. Exp. Med.* 188:561–575.
16. Okkenhaug, K., A. Bilancio, G. Farjot, H. Priddle, S. Sancho, E. Peskett, W. Pearce, S.E. Meek, A. Salpekar, M.D. Waterfield, et al. 2002. Impaired B and TCR signaling in p110delta PI 3-kinase mutant mice. *Science.* 297:1031–1034.
17. Borlado, L.R., C. Redondo, B. Alvarez, C. Jimenez, L.M. Criado, J. Flores, M.A.R. Marcos, C. Martínez-A, D. Balomenos, and A.C. Carrera. 2000. Increased PI3-kinase activity induces a lymphoproliferative disorder and contributes to tumor generation in vivo. *FASEB J.* 14:895–903.

18. Sasaki, T., J. Irie-Sasaki, R.G. Jones, A.J. Oliveira-dos-Santos, W.L. Stanford, B. Bolon, A. Wakeham, A. Itie, D. Bouchard, I. Kozieradzki, et al. 2000. Function of PI3Kgamma in thymocyte development, T cell activation, and neutrophil migration. *Science*. 287:1040–1046.
19. Rodríguez-Borlado, L., D.F. Barber, C. Hernandez, M.A. Rodriguez-Marcos, A. Sanchez, E. Hirsch, M. Wymann, C. Martinez-A, and A.C. Carrera. 2003. Phosphatidylinositol 3-kinase regulates the CD4/CD8 T cell differentiation ratio. *J. Immunol*. 170:4457–4482.
20. Astoul, E., C. Edmunds, D.A. Cantrell, and S.G. Ward. 2001. PI 3-K and T-cell activation: limitations of T-leukemic cell lines as signaling models. *Trends Immunol*. 22:490–496.
21. Kumar, A., T.D. Humphreys, K.N. Kremer, P.S. Bramati, L. Bradfield, C.E. Edgar, and K.E. Hedin. 2006. CXCR4 physically associates with the T cell receptor to signal in T cells. *Immunity*. 25:213–224.
22. Bondeva, T., L. Pirola, G. Bulgarelli-Leva, I. Rubio, R. Wetzker, and M.P. Wymann. 1998. Bifurcation of lipid and protein kinase signals of PI3Kgamma to the protein kinases PKB and MAPK. *Science*. 282:293–296.
23. Welch, H.C., W.J. Coadwell, L.R. Stephens, and P.T. Hawkins. 2003. Phosphoinositide 3-kinase-dependent activation of Rac. *FEBS Lett*. 546:93–97.
24. Miletic, A.V., M. Swat, K. Fujikawa, and W. Swat. 2003. Cytoskeletal remodeling in lymphocyte activation. *Curr. Opin. Immunol*. 15:261–268.
25. Jimenez, C., R.A. Portela, M. Mellado, J.M. Rodriguez-Frade, J. Collard, A. Serrano, C. Martínez-A., J. Avila, and A.C. Carrera. 2000. Role of the PI3K regulatory subunit in the control of actin organization and cell migration. *J. Cell Biol*. 151:249–262.
26. Morgan, M.M., C.M. Labno, G.A. Van Seventer, M.F. Denny, D.B. Straus, and J.K. Burkhardt. 2001. Superantigen-induced T cell:B cell conjugation is mediated by LFA-1 and requires signaling through Lck, but not ZAP-70. *J. Immunol*. 167:5708–5718.
27. Nombela-Arrieta, C., R.A. Lacalle, M.C. Montoya, Y. Kunisaki, D. Megias, M. Marques, A.C. Carrera, S. Mañes, Y. Fukui, C. Martínez-A, and J.V. Stein. 2004. Differential requirements for DOCK2 and phosphoinositide-3-kinase gamma during T and B lymphocyte homing. *Immunity*. 21:429–441.
28. Barber, D.F., A. Bartolomé, C. Hernández, J.M. Flores, C. Redondo, C. Fernández-Arias, M. Camps, T. Ruckle, M.K. Schwarz, S. Rodríguez, et al. 2005. PI3Kγ inhibition blocks glomerulonephritis and extends lifespan in a murine systemic lupus model. *Nat. Med*. 11:933–935.
29. Barber, D.F., A. Bartolome, C. Hernandez, J.M. Flores, C. Fernandez-Arias, L. Rodriguez-Borlado, E. Hirsch, M. Wymann, D. Balomenos, and A.C. Carrera. 2006. Class IB-phosphatidylinositol 3-kinase (PI3K) deficiency ameliorates IA-PI3K-induced systemic lupus but not T cell invasion. *J. Immunol*. 176:589–593.
30. Deane, J.A., M.G. Kharas, J.S. Oak, L.N. Stiles, J. Luo, T.I. Moore, H. Ji, C. Rommel, L.C. Cantley, T.E. Lane, and D.A. Fruman. 2007. T-cell function is partially maintained in the absence of class IA phosphoinositide 3-kinase signaling. *Blood*. 109:2894–2902.
31. Webb, L.M., E. Vigorito, M.P. Wymann, E. Hirsch, and M. Turner. 2005. Cutting edge: T cell development requires the combined activities of the p110gamma and p110delta catalytic isoforms of phosphatidylinositol 3-kinase. *J. Immunol*. 175:2783–2787.
32. Swat, W., V. Montgrain, T.A. Doggett, J. Douangpanya, K. Puri, W. Vermi, and T.G. Diacovo. 2006. Essential role of PI3Kdelta and PI3Kgamma in thymocyte survival. *Blood*. 107:2415–2422.
33. Leopoldt, D., T. Hanck, T. Exner, U. Maier, R. Wetzker, and B. Nurnberg. 1998. Gbetagamma stimulates phosphoinositide 3-kinase-gamma by direct interaction with two domains of the catalytic p110 subunit. *J. Biol. Chem*. 273:7024–7029.
34. Ward, S.G., S.C. Ley, C. MacPhee, and D.A. Cantrell. 1992. Regulation of D-3 phosphoinositides during T cell activation via the T cell antigen receptor/CD3 complex and CD2 antigens. *Eur. J. Immunol*. 22:45–49.
35. Stanners, J., P.S. Kabouridis, K.L. McGuire, and C.D. Tsoukas. 1995. Interaction between G proteins and tyrosine kinases upon T cell receptor.CD3-mediated signaling. *J. Biol. Chem*. 270:30635–30642.
36. Monks, C.R., B.A. Freiberg, H. Kupfer, N. Sciaky, and A. Kupfer. 1998. Three-dimensional segregation of supramolecular activation clusters in T cells. *Nature*. 395:82–86.
37. Grakoui, A., S.K. Bromley, C. Sumen, M.M. Davis, A.S. Shaw, P.M. Allen, and M.L. Dustin. 1999. The immunological synapse: a molecular machine controlling T cell activation. *Science*. 285:221–227.
38. Dustin, M.L., and A.C. Chan. 2000. Signaling takes shape in the immune system. *Cell*. 103:283–294.
39. Holsinger, L.J., I.A. Graef, W. Swat, T. Chi, D.M. Bautista, L. Davidson, R.S. Lewis, F.W. Alt, and G.R. Crabtree. 1998. Defects in actin-cap formation in Vav-deficient mice implicate an actin requirement for lymphocyte signal transduction. *Curr. Biol*. 8:563–572.
40. Wulfing, C., M.D. Sjaastad, and M.M. Davis. 1998. Visualizing the dynamics of T cell activation: intracellular adhesion molecule 1 migrates rapidly to the T cell/B cell interface and acts to sustain calcium levels. *Proc. Natl. Acad. Sci. USA*. 95:6302–6307.
41. Etienne-Manneville, S., and A. Hall. 2002. Rho GTPases in cell biology. *Nature*. 420:629–635.
42. Ma, A.D., A. Metjian, S. Bagrodia, S. Taylor, and C.S. Abrams. 1998. Cytoskeletal reorganization by G protein-coupled receptors is dependent on phosphoinositide 3-kinase gamma, a Rac guanosine exchange factor, and Rac. *Mol. Cell. Biol*. 18:4744–4751.
43. Weiss-Haljiti, C., C. Pasquali, H. Ji, C. Gillieron, C. Chabert, M.L. Curchod, E. Hirsch, A.J. Ridley, R.H. van Huijsduijnen, M. Camps, and C. Rommel. 2004. Involvement of phosphoinositide 3-kinase gamma, Rac, and PAK signaling in chemokine-induced macrophage migration. *J. Biol. Chem*. 279:43273–43284.
44. Fischer, K.D., Y.Y. Kong, H. Nishina, K. Tedford, L.E. Marengere, I. Kozieradzki, T. Sasaki, M. Starr, G. Chan, S. Gardener, et al. 1998. Vav is a regulator of cytoskeletal reorganization mediated by the T-cell receptor. *Curr. Biol*. 8:554–562.
45. Prisco, A., L. Vanes, S. Ruf, C. Trigueros, and V.L. Tybulewicz. 2005. Lineage-specific requirement for the PH domain of Vav1 in the activation of CD4+ but not CD8+ T cells. *Immunity*. 23:263–274.
46. Hirsch, E., V.L. Katanaev, C. Garlanda, O. Azzolino, L. Pirola, L. Silengo, S. Sozzani, A. Mantovani, F. Altruda, and M.P. Wymann. 2000. Central role for G protein-coupled phosphoinositide 3-kinase gamma in inflammation. *Science*. 287:1049–1053.
47. Seder, R.A., W.E. Paul, M.M. Davis, and B. Fazekas de St. Groth. 1992. The presence of interleukin 4 during in vitro priming determines the lymphokine-producing potential of $CD4^+$ T cells from T cell receptor transgenic mice. *J. Exp. Med*. 176:1091–1098.
48. Mamalaki, C., J. Elliott, T. Norton, N. Yannoutsos, A.R. Townsend, P. Chandler, E. Simpson, and D. Kioussis. 1993. Positive and negative selection in transgenic mice expressing a T-cell receptor specific for influenza nucleoprotein and endogenous superantigen. *Dev. Immunol*. 3:159–174.